Tactile length contraction as Bayesian inference

Jonathan Tong, Vy Ngo and Daniel Goldreich

J Neurophysiol 116:369-379, 2016. First published 27 April 2016;
doi: 10.1152/jn.00029.2016

J Neurophysiol 116: 369–379, 2016.
First published April 27, 2016; doi:10.1152/jn.00029.2016.

Tactile length contraction as Bayesian inference

Jonathan Tong,[1] Vy Ngo,[1] and Daniel Goldreich[1,2,3]

[1]*Department of Psychology, Neuroscience and Behaviour, McMaster University, Hamilton, Ontario, Canada;* [2]*McMaster Integrative Neuroscience Discovery and Study, Hamilton, Ontario, Canada; and* [3]*McMaster University Origins Institute, Hamilton, Ontario, Canada*

Submitted 11 January 2016; accepted in final form 24 April 2016

Tong J, Ngo V, Goldreich D. Tactile length contraction as Bayesian inference. *J Neurophysiol* 116: 369–379, 2016. First published April 27, 2016; doi:10.1152/jn.00029.2016.—To perceive, the brain must interpret stimulus-evoked neural activity. This is challenging: The stochastic nature of the neural response renders its interpretation inherently uncertain. Perception would be optimized if the brain used Bayesian inference to interpret inputs in light of expectations derived from experience. Bayesian inference would improve perception on average but cause illusions when stimuli violate expectation. Intriguingly, tactile, auditory, and visual perception are all prone to length contraction illusions, characterized by the dramatic underestimation of the distance between punctate stimuli delivered in rapid succession; the origin of these illusions has been mysterious. We previously proposed that length contraction illusions occur because the brain interprets punctate stimulus sequences using Bayesian inference with a low-velocity expectation. A novel prediction of our Bayesian observer model is that length contraction should intensify if stimuli are made more difficult to localize. Here we report a tactile psychophysical study that tested this prediction. Twenty humans compared two distances on the forearm: a fixed reference distance defined by two taps with 1-s temporal separation and an adjustable comparison distance defined by two taps with temporal separation $t \leq 1$ s. We observed significant length contraction: As t was decreased, participants perceived the two distances as equal only when the comparison distance was made progressively greater than the reference distance. Furthermore, the use of weaker taps significantly enhanced participants' length contraction. These findings confirm the model's predictions, supporting the view that the spatiotemporal percept is a best estimate resulting from a Bayesian inference process.

Bayesian inference; sensory saltation; somatosensory psychophysics; spatial illusion; uncertainty

NEW & NOTEWORTHY

A growing body of evidence—particularly from visual research—has suggested that perception may be a Bayesian best guess, in which the brain interprets imprecise sensory inputs in light of expectations forged from experience. Passive tactile perception has rarely been studied from a Bayesian perspective. Here we show that the perception of tactile spatiotemporal stimuli conforms to the predictions of a Bayesian observer model that incorporates a low-velocity expectation.

HUMANS TAKE FOR GRANTED the ability to perceive the external world, but how does the nervous system accomplish this remarkable feat? The response of a cortical sensory neuron to a repeated identical stimulus typically shows considerable trial-by-trial variability, characterized by Poisson-like statistics (Shadlen and Newsome 1998; Sripati et al. 2006). Consequently, the neural activity observed on a given trial could have resulted from any one of many different stimuli. For this reason, even apparently simple perceptual tasks, such as that of localizing a tap to the skin, are fraught with uncertainty (Fig. 1). Viewed statistically, perception involves the notoriously challenging "inverse problem" (Pizlo 2001) of inferring a cause (e.g., the location of a stimulus) from its stochastically generated effects (e.g., evoked neural activity). This challenge is optimally met via Bayesian inference (Knill and Pouget 2004; Ma et al. 2006; Penny 2012; Vincent 2015).

A Bayesian observer interprets imprecise sensory data in light of expectations derived from experience. Specifically, for each possible stimulus the Bayesian observer considers two probabilities: *1*) the probability of the sensory data, given the stimulus (the likelihood), and *2*) the prevalence of the stimulus, learned from experience (the prior). The product of these probabilities is proportional to the posterior probability of the stimulus. The Bayesian observer selects a particular stimulus—e.g., the one with highest posterior probability—as the percept (Yuille and Bülthoff 1996). Bayesian inference optimizes perceptual performance on average but is expected to cause illusions when stimuli violate expectation; therefore, the study of illusions can be used to test Bayesian observer models (Geisler and Kersten 2002).

Intriguingly, tactile, auditory, and visual perception are all prone to length contraction illusions, characterized by the dramatic underestimation of the distance between stimuli delivered in rapid succession (Goldreich 2007). Much empirical work has characterized tactile length contraction illusions, which include the famous cutaneous rabbit illusion (Asai and Kanayama 2012; Blankenburg et al. 2006; Cholewiak 1999; Geldard 1982; Geldard and Sherrick 1972; Helson 1930; Kilgard and Merzenich 1995; Lechelt and Borchert 1977; Marks et al. 1982; Miyazaki et al. 2010; Trojan et al. 2014). In the cutaneous rabbit illusion, a sequence of taps delivered in rapid succession to as few as two skin locations evokes the sensation of taps hopping progressively along the arm from the first location to the next; the illusory percept thus includes the vivid perception of taps landing on areas of the skin that were never in fact stimulated (Geldard 1982). Two key findings from empirical studies of tactile length contraction are that perceived intertap distance grows approximately linearly with the actual distance (Cholewiak 1999; Marks et al. 1982), but nonlinearly with the time (Kilgard and Merzenich 1995), between taps to the skin.

We previously proposed a Bayesian observer model that provides a unified explanation for these findings and repro-

Address for reprint requests and other correspondence: D. Goldreich, Dept. of Psychology, Neuroscience and Behaviour, McMaster Univ., 1280 Main St. W., Hamilton, ON L8S 4K1, Canada (e-mail: goldrd@mcmaster.ca).

duces a variety of length contraction illusions (Goldreich 2007; Goldreich and Tong 2013). The Bayesian observer assumes that taps presented in rapid sequence along the skin originate from a single moving source. Each tap evokes a noisy internal position measurement drawn from a Gaussian distribution centered on the actual tap position, with spatial standard deviation (SD) σ_s. To perceive the spatial separation between successive taps, the Bayesian observer interprets the position measurements in light of a low-velocity expectation, a Gaussian prior centered on zero velocity, with SD σ_v. Consequently, taps separated by a large distance and a short time (a fast movement) are misjudged as separated by a shorter distance, a perceptual interpretation that favors low speeds (Fig. 2*A*).

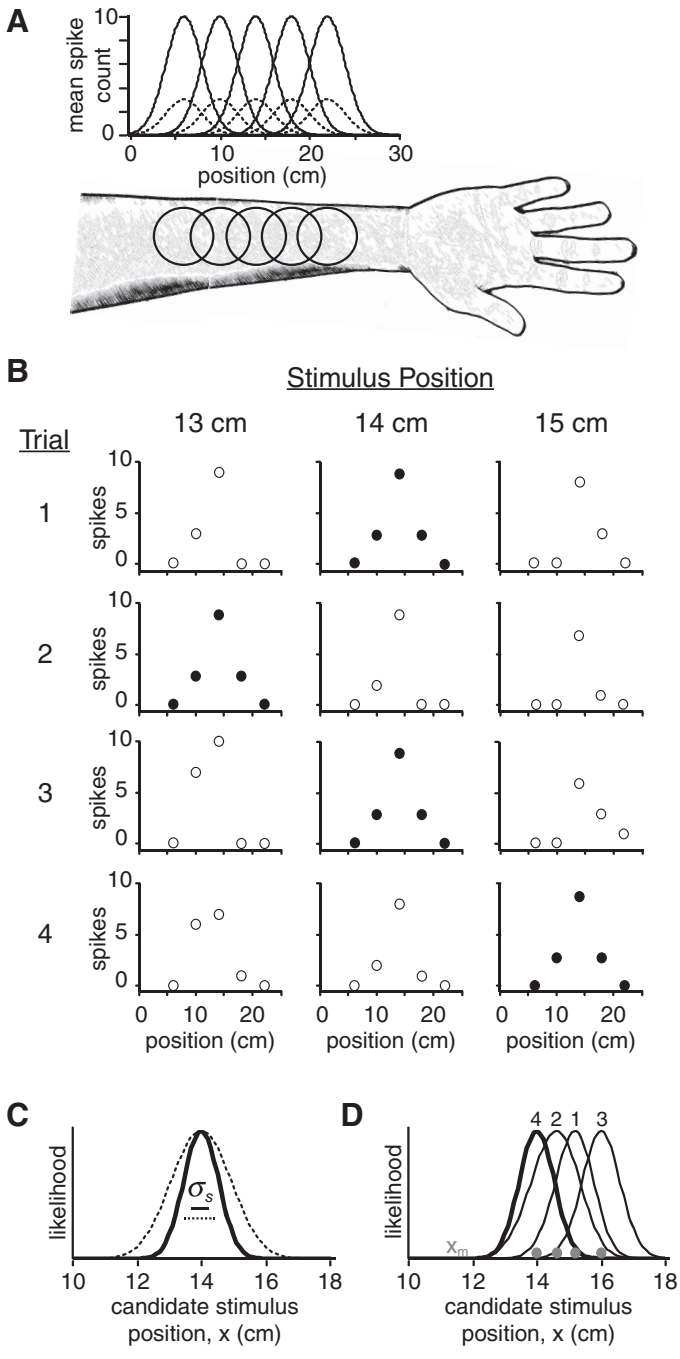

The Bayesian observer's distance percept, l^*, is given by the perceptual length contraction formula, in which the ratio $\tau = \sigma_s/\sigma_v$ defines a time constant for space perception (Fig. 2*B*). The Bayesian observer reproduces both the linear effect of space (Fig. 2, *C* and *D*, *top*) and the nonlinear effect of time (Fig. 2, *C* and *D*, *middle*) on perceived length. Importantly, the model also predicts that sequences of particularly difficult-to-localize taps (greater σ_s) will give rise to more pronounced length contraction (smaller l^*; Fig. 2, *C* and *D*, *bottom*). Here we tested this novel prediction by presenting human participants with sequences of taps that indented the skin either weakly or strongly. The results confirmed the model's prediction, supporting the hypothesis that the tactile spatiotemporal percept is a probabilistic inference.

MATERIALS AND METHODS

Participants

Thirty individuals (18–34 yr old, median age 21.9 yr; 13 men, 17 women) were recruited from the McMaster University community. By self-report, all participants were free of conditions known to adversely affect the sense of touch (e.g., diabetes, carpal tunnel syndrome, calluses, or injuries on tested skin areas) or perceptual processing (dyslexia, attention deficit disorder, learning disability, or central nervous system disorders). Each participant provided signed informed consent. The McMaster University Research Ethics Board approved all procedures. Of the initial 30 recruits, 20 passed the perceptual qualification criteria (see below) and completed the full battery of psychophysical tests. We report the data from those 20 participants (18–34 yr old, median age 21.6 yr; 10 men, 10 women).

Stimulus Delivery

We used a precision tactile stimulus system (Tactile Stimulator MkII; Fong Engineering, Oakland, CA) to deliver submillimeter

Fig. 1. Single-tap localization uncertainty. *A*: circles depict receptive fields of 5 simulated cortical neurons, with centers at 6, 10, 14, 18, and 22 cm on the arm. Plots: mean firing (spike counts) of the neurons in response to a brief tap of large (solid curve) or small (dashed curve) amplitude, delivered at each position along the arm. These tuning curves are Gaussian functions with SD 2 cm; the actual shapes, sizes, and activity profiles of cortical receptive fields are much more variable than those shown (Peters et al. 2015). *B*: responses of the simulated neurons to 12 large-amplitude stimulus presentations: 4 repetitions each at positions 13, 14, and 15 cm on the arm. Each panel plots spike count (*y*-axis) against receptive field center position (*x*-axis). Spike counts vary stochastically from trial to trial, even when stimulus position is held constant. Consequently, stimuli at different positions can produce identical population responses (plots with filled data points: 0, 3, 9, 3, and 0 spikes in the 5 neurons). *C*: the likelihood function (LF) plots the probability of an observed response, given each possible stimulus position. Solid curve: normalized LF for 0, 3, 9, 3, 0 spikes. The SD of the LF, σ_s (solid horizontal line), indicates the observer's spatial uncertainty regarding the tap position. This LF is maximal at 14 cm, as the observed response occurs with greatest frequency for a stimulus at that position. Dashed curve: normalized LF for a plausible weak-tap response: 0, 1, 3, 1, 0 spikes (made by scaling the strong-tap response in each neuron by one-third). This LF is also peaked at 14 cm but has greater σ_s (dashed horizontal line); on this basis, we predicted that weaker taps would result in greater spatial uncertainty. We computed each LF under the assumption that the neurons' spike counts are subject to independent Poisson variability (Ma et al. 2006). *D*: LFs for the 4 population responses shown in *B*, *right*. Upon repeated identical stimulus presentations at 15 cm, the LF jitters stochastically, reflecting the variability in the population response; the number above each plot refers to the trial number in *B*. Equivalent LF shape and jitter would result if on each trial a stimulus-evoked position measurement, x_m (gray dots), were drawn from a Gaussian distribution centered on 15 cm with SD = σ_s. For mathematical convenience, our Bayesian observer model incorporates such position measurements in lieu of neural population activity.

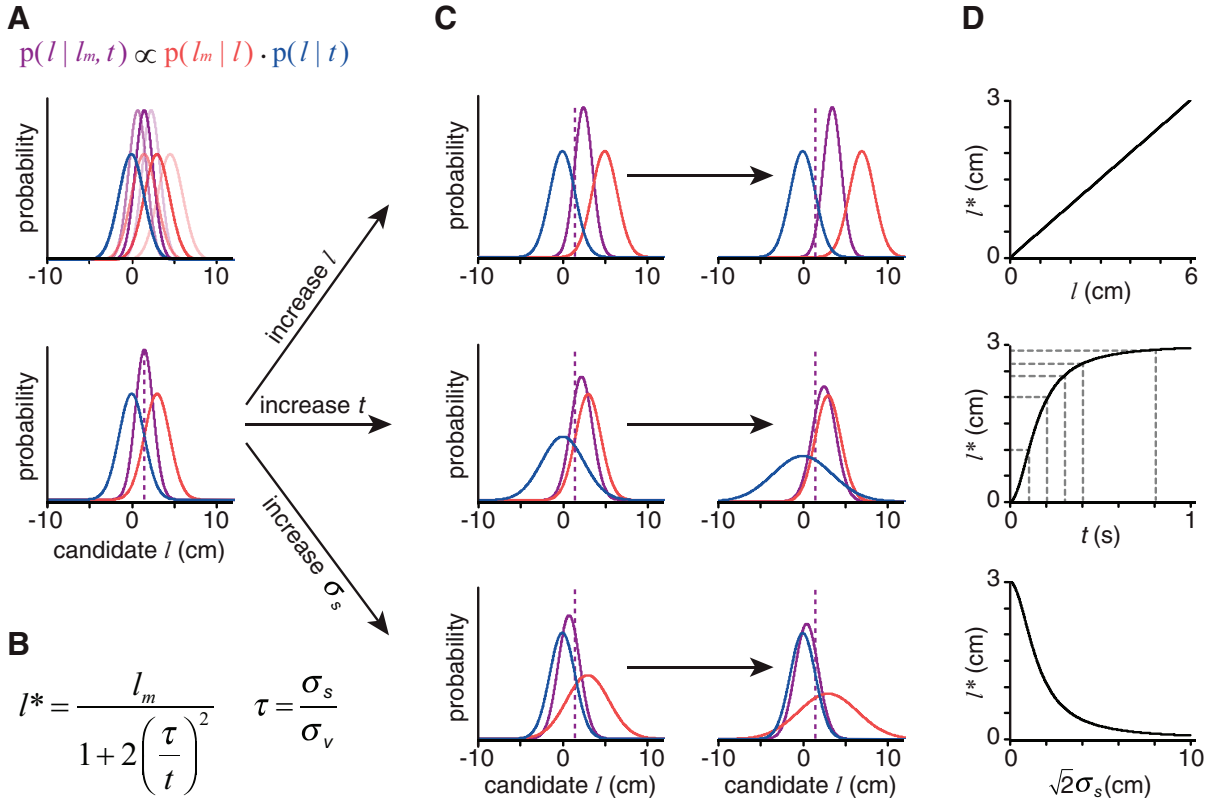

Fig. 2. Bayesian observer model. *A*, *top*: the Bayesian observer is presented with repeated trials in which 2 taps contact the skin with spatiotemporal separation l = 3 cm, t = 0.15 s. Each tap evokes a position measurement, x_m, that varies stochastically around the true tap location with SD = σ_s (see Fig. 1*D*). The observer therefore experiences a length measurement, $l_m = x_{1m} - x_{2m}$, that varies stochastically around the true length (3 cm) with SD = $\sigma_s\sqrt{2}$. On each trial, the length measurement results in a likelihood function (red) with mode = l_m and SD = $\sigma_s\sqrt{2}$. The observer has a low-velocity expectation, equivalent to a prior distribution over length (blue) with mode = 0 cm and SD = $t\sigma_v$ (see Eq. A8 of Goldreich and Tong 2013). In the examples shown, $\sigma_s\sqrt{2}$ = 1.5 cm and σ_v = 10 cm/s. On each trial, the observer multiplies its likelihood function by its prior distribution to obtain a posterior distribution (purple). Bayes' formula (*inset*) shows the calculation. *Bottom*: averaged over repeated trials, the mode of likelihood function equals l, but the mode of the posterior (the percept, l^*) underestimates l. Here, l^* = 1.5 cm (vertical dashed line). *B*: l^* is related to l_m and t via by the perceptual length contraction formula (for derivation, see Goldreich and Tong 2013). τ, a time constant for spatial perception, is equal to σ_s/σ_v. *C*: effect of length, time, and spatial uncertainty manipulation on l^* (the mode of the posterior). In each case, 1 variable was manipulated while the other 2 were held at the same value as in *A*. *Top*: increasing l (*left*: l = 5 cm; *right*: l = 7 cm) shifts the likelihood function, causing a linear increase in l^* (*left*: l^* = 2.5 cm; *right*: l^* = 3.5 cm). *Middle*: increasing t (*left*: t = 0.25 s; *right*: t = 0.35 s) broadens the prior, causing a nonlinear increase in l^* (*left*: l^* = 2.21 cm; *right*: l^* = 2.53 cm). *Bottom*: the model predicts that increasing σ_s (*left*: $\sigma_s\sqrt{2}$ = 2.5 cm; *right*: $\sigma_s\sqrt{2}$ = 3.5 cm) will broaden the likelihood function, thereby causing a reduction in l^* (*left*: l^* = 0.79 cm; *right*: l^* = 0.47 cm). For reference, the vertical dashed lines in each panel are replicas of the vertical dashed line in *A*, *bottom*. *D*: l^* plotted against l (*top*), t (*middle*), and $\sigma_s\sqrt{2}$ (*bottom*). Dashed lines (*middle*) show, as indicated by the length contraction formula (*B*), that l^*/l = 1/3, 2/3, 9/11, 8/9, and 32/33 (i.e., 33, 66, 81, 88, and 96/99) when t = τ, 2τ, 3τ, 4τ, and 8τ, respectively (here, τ = 106 ms). The prediction that l^* will decrease when σ_s increases (*bottom*) is also apparent from the length contraction formula (*B*).

mechanical stimuli orthogonally against the skin surface. The MkII system controlled three cylindrical motors independently. Precision micromanipulators (Eric Sobotka) held the motors and allowed for angular and three-axis translational position adjustments. Each motor was equipped with a linear variable displacement transducer for real-time displacement readout. Attached to the shaft of each motor was a steel domed pinhead probe tip, 1 mm in diameter, that made contact with the skin.

We programmed a Mac Pro 3.1 computer (Apple) in LabVIEW (National Instruments) to communicate (via DAQ PCIe-6259, 16-bit analog output; National Instruments) with the MkII system. The program outputted a single-period 10-ms square wave or sine wave command voltage pulse to produce a strong or weak stimulus, respectively. Inertia of the probe and the mechanical properties of the skin resulted in the actual movements depicted in Fig. 3*A*. Peak displacement amplitude into the skin was approximately twice as large for the strong (~170 μm) as for the weak (~85 μm) stimulus. Peak displacement velocity into the skin was similarly twice as large for the strong (~60 μm/ms) as for the weak (~30 μm/ms) stimulus. The strong stimulus produced the sensation of a single abrupt and firm tap; the weak stimulus produced the sensation of a single abrupt but noticeably softer tap.

The participant was seated comfortably facing a table on which the experimental apparatus was concealed by an opaque black curtain. The participant's right forearm was inserted under the curtain and rested, palm side up, below the stimulus probes. To aid the experimenter in probe positioning, the forearm was demarcated with a fine-tipped pen at 0.5-cm intervals, starting ~5 cm proximal to the wrist and progressing proximally. We avoided placing probes closer than 5 cm to the wrist, because the wrist has high spatial acuity and may serve as a perceptual anchor point (Cholewiak and Collins 2003; Cody et al. 2008); indeed, pilot experiments revealed a reduction in perceptual length contraction when stimuli were placed near the wrist. To initiate length comparison testing (below), the experimenter lowered the three probes to a baseline skin indentation of 0.5 mm. The experimenter then triggered taps individually through each probe and queried the participant as to their relative perceived strengths. If taps through a particular probe felt weaker than taps through the others, the probe was lowered in 100-μm increments until subjective equality of stimulus intensity was achieved. A sound conditioner (Marsona

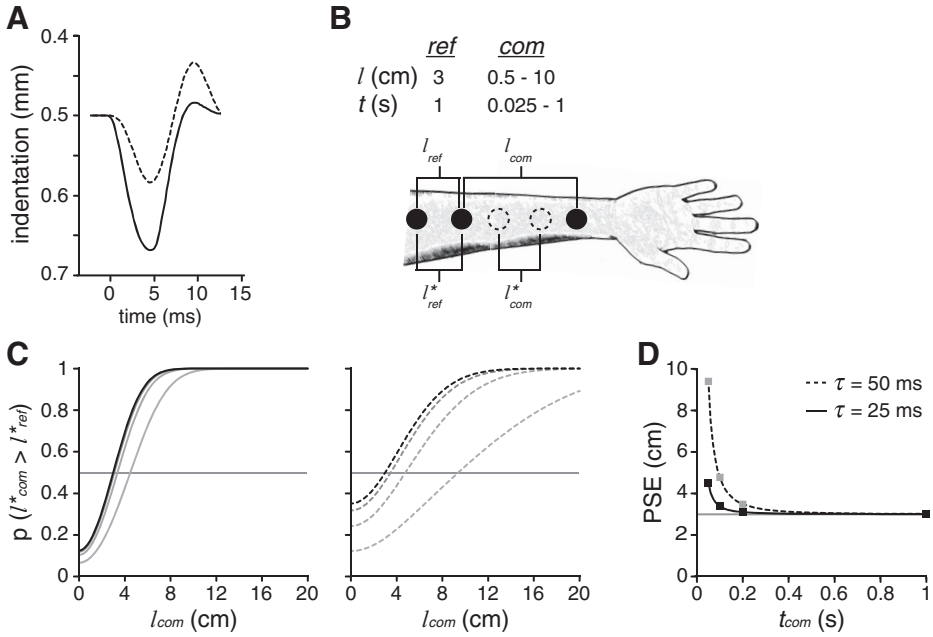

Fig. 3. Tactile stimuli, perceptual task, and predicted results. *A*: stimulus waveforms used to produce strong (solid curve) and weak (dashed curve) taps. Downward corresponds to displacement into the skin. The probe had a baseline indentation of 0.5 mm. Stimulus onset occurred at *time 0*. *B*: 2-interval forced-choice (2-IFC) length comparison experiment. Reference length and time (l_{ref} and t_{ref}) were fixed at 3 cm (center-to-center probe distance) and 1 s (stimulus onset asynchrony). Comparison length and time (l_{com} and t_{com}) were varied. On each trial, participants reported which of the 2 perceived spatial separations, l^*_{com} or $l^*_{ref,}$ was longer. When t_{com} was small, considerable perceptual length contraction occurred, making l^*_{com} (dashed circles) much smaller than l_{com}. In contrast, l^*_{ref} approximated l_{ref}, because t_{ref} was large (1 s). *C*: Bayesian observer's psychometric functions when spatial uncertainty was low (*left*, solid curves) or high (*right*, dashed curves). For the examples shown, σ_s was set to 1 cm (*left*) or 2 cm (*right*); σ_v was held constant at 40 cm/s. Curves (darker to lighter) correspond to t_{com} = 1,000, 200, 100, and 50 ms. The l_{com} at which each curve has height 0.5 (horizontal line) is the point of subjective equality (PSE; l_{com} value at which $l^*_{com} = l^*_{ref}$ on average). *D*: the PSEs extracted from *C* are plotted against t_{com} for the low (solid curve, black squares)- and high (dashed curve, gray squares)-spatial uncertainty conditions. Horizontal line: PSE = 3 cm (i.e., l_{ref}). *Inset*: $\tau = \sigma_s/\sigma_v$.

1288A; Marpac) played white noise to mask any audible motor sounds.

Sensory Testing

We tested participants on a battery of two-interval forced-choice (2-IFC) length comparison experiments in order to assess both their spatial acuity and the extent to which they experienced perceptual length contraction. The participant judged which was greater: a variable comparison length, l_{com} (taps delivered successively by distal and middle probes, with temporal separation t_{com}), or a fixed 3-cm reference length, l_{ref} (taps delivered successively by proximal and middle probes, with temporal separation t_{ref} = 1,000 ms) (Fig. 3*B*). The presentation order of the reference and comparison pairs, as well as the stimulus order of the taps making up each pair, was randomized in each trial. The participant indicated by button press with the left hand whether the pair with the longer separation length occurred first or second. We used an adaptive psychophysics procedure (see below) to efficiently estimate the participant's psychometric function: the proportion of trials in which l_{com} was judged to be longer than l_{ref}, as a function of l_{com}.

For each tap strength, participants first completed a testing block (*block 1*) in which t_{com} and t_{ref} were identical (i.e., t_{com} = 1,000 ms). Performance on this block was used to derive a spatial acuity measure, the just-noticeable difference (JND) between l_{com} and l_{ref}. Participants next completed four testing blocks (*blocks 2–5*) with $t_{com} < 1{,}000$ ms. Performance on each of the five blocks was used to extract the comparison length that the participant reported feeling longer than the reference length with 50% probability: the point of subjective equality (PSE). *Block 2* used t_{com} = 200 ms. The PSE typically increased above 3 cm as t_{com} was decreased, indicating the presence of perceptual length contraction. For some participants, small t_{com} values resulted in considerable length contraction, such that the PSE was >10 cm, the maximum comparison separation achievable by our stimulus apparatus. Therefore, to avoid ceiling effects, we used the following rule to determine each subsequent t_{com}: Upon completion of a block, if the participant's PSE was <10 cm, t_{com} was reduced by half; if the participant's PSE was >10 cm, t_{com} was increased halfway to its value on the previous block. The sequence of t_{com} (*blocks 2–5*) for participants who completed all blocks with PSE < 10 cm was 200, 100, 50, and 25 ms.

Adaptive psychophysics. To conduct the testing, we used the psi adaptive procedure (modified from Kontsevich and Tyler 1999). Each block comprised 100 trials consisting of ten 10-trial segments. Within each segment, l_{com} was held constant; prior to the segment, the psi procedure instructed the experimenter to apply the l_{com} expected to maximize the information gain regarding the participant's psychometric function (i.e., the l_{com} that minimized the expected entropy of the joint posterior over psychometric function parameters). Each block lasted ~27 min; a rest period of ~3 min occurred halfway through the block.

We parameterized the psychometric function as a Weibull function (Klein 2001) with position parameter a, slope parameter b, and lapse-rate parameter ε. An advantage of using the Weibull function is that this method allowed us to derive measures of participant performance (JND and PSE) that were not based on our Bayesian observer model. These model-independent estimates could later be compared to the performance of the Bayesian observer. The Weibull function took the form

$$p(l^*_{com} > l^*_{ref} \,|\, l_{com}) = (1-\varepsilon)\left(1 - 2^{-(l_{com}/a)^b}\right) + \frac{\varepsilon}{2} \qquad (1)$$

We initiated the psi procedure with uniform prior probabilities over a range of a (0.1–10 cm, widened to 0.1–20 cm for off-line analysis),

b (0.2–5), and ε (0.01–0.08). After completion of each t_{com} = 1,000 ms testing block, we marginalized the joint (a, b, ε) posterior over ε to find the MAP estimate psychometric function, from which we read out the l_{com} resulting in $p(l^*_{com} > l^*_{ref}) = 0.75$. We subtracted l_{ref} (i.e., 3 cm) from this value to find the participant's JND. The JND divided by l_{ref} was the participant's Weber fraction. For all testing blocks, we marginalized the joint (a, b, ε) posterior over b and ε to extract the posterior over a, from which we read out the mode as the best estimate of the participant's PSE.

Order of experiments. For the majority of participants, testing occurred over 3 (not necessarily sequential) days, with visits of ~2 h per day. On *day 1*, participants completed four testing blocks: one block each of point localization experiments (see *Assessing perceptual stability*) for strong and weak stimuli (order counterbalanced) followed by one block each of length comparison experiments with t_{com} = 1,000 ms for strong and weak stimuli (order counterbalanced). Participants who qualified on these tasks (see below) were permitted to continue on to *days 2* and *3*. On *day 2*, they completed four length comparison blocks with $t_{com} < 1{,}000$ ms followed by one block of point localization; *day 2* experiments used either exclusively strong or exclusively weak stimuli. *Day 3* followed the same layout as *day 2*, with stimuli exclusively of the other stimulus strength. The *day 2-day 3* stimulus strength order (strong-weak or weak-strong) was counterbalanced. Four participants completed a more extensive testing battery that required 12 days and consisted of multiple repetitions of the point localization task, length comparison tasks with varying l_{ref}, and testing on finger as well as forearm. For those four participants, we include here only the forearm, 3.0 cm reference data, in keeping with the protocol used for the other 16 participants. We shifted to the 3-day protocol after testing those four participants, in order to make the experiment more manageable for participants and experimenters.

Qualification criteria. To ensure that participants were able to concentrate well and provide reliable baseline data, we required that their *day 1* performance pass two qualification criteria. *1*) We calculated a guessing Bayes factor: the probability of the performance data given that the participant was guessing randomly on every trial divided by the probability that the participant's responses followed a best-fit psychometric function; we required that this Bayes factor not exceed 0.001 on either the point localization or the length comparison blocks. *2*) We required that the participant's PSE at t_{com} = 1,000 ms differ by no more than 1 cm from the reference separation of 3 cm, indicating that the participant was able to reliably compare two spatial separations of equal temporal interval. Provided these criteria were met on each of the four *day 1* testing blocks, participants continued testing. If participants failed to meet criterion on any testing block, they were given a second chance (an extra testing block) and were disqualified from the study if they again failed to meet criterion. In total, 10 participants (of the 30 recruited to the study) were disqualified: 2 participants failed only *criterion 1*; 4 failed only *criterion 2*; and 4 failed both criteria. The disqualified participants presumably had difficulty concentrating and/or had spatial acuity insufficient to perceive accurately a 3-cm distance between taps.

Assessing perceptual stability. To test for the presence of practice effects, we conducted a simple 2-IFC point localization task on the first and final days of testing with each stimulus strength: the participant felt two taps, separated by 500 ms, at different locations on the forearm (order randomized) and responded by button press to answer the question, "Did the tap closer to the wrist come first or second?" We used the psi adaptive procedure to estimate the participant's psychometric function (proportion correct as a function of the spatial separation between taps), from which we extracted the 75%-correct separation. The results indicated that performance was stable across testing days: a 2 × 2 repeated-measures ANOVA with tap strength (strong and weak) and testing day (first and final) as factors indicated a highly significant effect of tap strength ($F_{1,19}$ = 133.206, $P = 5 \times 10^{-10}$) but no effect of testing day ($F_{1,19}$ = 0.012, P = 0.915) and no interaction ($F_{1,19}$ = 1.380, P = 0.255).

Bayesian Observer Fitting

To compare human performance to that of the Bayesian observer, we first determined the performance of the Bayesian observer on the same perceptual tasks completed by the human participants for a wide range of parameter values. We next found the parameter values for the Bayesian observer that best fit each human participant.

Generating the Bayesian observer's length comparison psychometric function. The Bayesian observer's psychometric function for each t_{com} is the proportion of trials on which it perceives l_{com} to be greater than l_{ref}, plotted against l_{com}: $\psi_{model}(l_{com})$. The Bayesian observer's percepts for reference and comparison distances are normally distributed, with means and SDs resulting from the perceptual length contraction formula:

$$\mu_{l^*_{com}} = \frac{l_{com}}{1 + 2\left(\frac{\tau}{t_{com}}\right)^2} \qquad \sigma^2_{l^*_{com}} = \frac{2\sigma_s^2}{\left(1 + 2\left(\frac{\tau}{t_{com}}\right)^2\right)^2}$$
$$\mu_{l^*_{ref}} = \frac{3\text{ cm}}{1 + 2\left(\frac{\tau}{1{,}000\text{ ms}}\right)^2} \qquad \sigma^2_{l^*_{ref}} = \frac{2\sigma_s^2}{\left(1 + 2\left(\frac{\tau}{1{,}000\text{ ms}}\right)^2\right)^2} \quad (2)$$

Note that l^* can take on negative or positive values. A negative value would indicate a perceptual spatial reversal in which the more distal tap was perceived to be more proximal. However, the participants' task was to judge only which tap pair had longer spatial separation. Therefore, to determine the Bayesian observer's psychometric function, we used the percept distributions (*Eqs. 2*) to calculate the probability that the absolute value of l^*_{com} was greater than the absolute value of l^*_{ref}:

$$\begin{aligned}\psi_{model}(l_{com}) &= p\left(\text{abs}\left(l^*_{com}\right) > \text{abs}\left(l^*_{ref}\right) \middle| l_{com}\right)\\ &= \int_{-\infty}^{\infty} p\left(l^*_{ref} \middle| (\mu, \sigma^2)_{l^*_{ref}}\right)\Big[p\left(l^*_{com} > \left|l^*_{ref}\right| \middle| (\mu, \sigma^2)_{l^*_{com}}\right)\\ &\quad + p\left(l^*_{com} < -\left|l^*_{ref}\right| \middle| (\mu, \sigma^2)_{l^*_{com}}\right)\Big] dl^*_{ref} \quad (3)\end{aligned}$$

The psychometric function, and consequently the PSE, depended on the Bayesian observer's parameter settings—its spatial uncertainty (σ_s) and low-speed expectation (σ_v)—as well as t_{com} (Fig. 3, *C* and *D*).

Fitting the Bayesian observer to human performance. We next asked whether the Bayesian observer, with a single σ_s and σ_v, could match a human participant's performance across all t_{com} blocks of one tap strength. For each human, we modeled the psychometric function, $\psi(l_{com})$, as a mixture of the Bayesian observer's psychometric function and a lapse rate term:

$$\psi(l_{com}) = (1 - \varepsilon)\psi_{model}(l_{com}) + \frac{\varepsilon}{2} \quad (4)$$

For each combination of 50 σ_s values (range 0.1–5.0 cm), 100 σ_v values (range 1–100 cm/s), and 8 ε values (range 0.01–0.08), we calculated the likelihood:

$$p(d \mid \sigma_s, \sigma_v, \varepsilon) = \prod_{t_{com}} \prod_{l_{com}} \psi^{n_{com}}_{t_{com}, l_{com}, \sigma_s, \sigma_v, \varepsilon}\left(1 - \psi_{t_{com}, l_{com}, \sigma_s, \sigma_v, \varepsilon}\right)^{n_{ref}} \quad (5)$$

This is the probability, given σ_s, σ_v, and ε, of the participant's complete behavioral data set (d) at a given tap strength: for every comparison length and time, the number of trials in which the comparison length was perceived to be longer than the reference (n_{com}) and the number of trials in which the reference was perceived to be longer than the comparison (n_{ref}). Beginning with a uniform prior over σ_s, σ_v, and ε, we used Bayes' rule to find the joint (σ_s, σ_v, ε) posterior. We marginalized this over ε to obtain the joint (σ_s, σ_v) posterior. We read out the mode to obtain our best estimates for these parameters, from which we calculated the best estimate $\tau = \sigma_s/\sigma_v$.

Statistical Analysis

For frequentist analyses on point-estimate data, we used SPSS Statistics v.22 (IBM) to conduct two-tailed paired *t*-tests and repeated-measures ANOVAs (type III sum of squares, with Greenhouse-Geisser correction in cases of violation of sphericity as indicated by a significant Mauchly's test).

We additionally used Bayesian data analyses to more thoroughly probe two questions of fundamental importance to the study. First, for each t_{com}, we calculated the posterior probability that the mean PSE across participants in the weak-tap condition was greater than that in the strong-tap condition. To account for variability both between and within participants, we implemented a hierarchical model that represented participants' PSEs at each t_{com} and tap strength as lognormally distributed with unknown location (μ) and scale (σ) parameters:

$$p(\mathrm{PSE} \mid \mu, \sigma) = \frac{1}{(\mathrm{PSE})\sigma\sqrt{2\pi}} \exp\left(-\frac{(\ln \mathrm{PSE} - \mu)^2}{2\sigma^2}\right) \quad (6)$$

The probability of an individual participant's data, d_i (at each l_{com}, the number of trials on which the comparison length was perceived as longer and the number of trials on which the reference length was perceived as longer), given (μ, σ), was

$$p(d_i \mid \mu, \sigma) = \int_{\mathrm{PSE}} p(d_i \mid \mathrm{PSE}) p(\mathrm{PSE} \mid \mu, \sigma) d\mathrm{PSE} \quad (7)$$

where the first factor in the integrand was proportional to the posterior over the Weibull function *a* parameter (because we used a uniform prior; see *Adaptive psychophysics*). The probability of all participants' data (D: d_1, d_2,..., d_{20}) at a particular t_{com} and tap strength, given (μ, σ), was

$$p(D \mid \mu, \sigma) = \prod_i p(d_i \mid \mu, \sigma) \quad (8)$$

For each t_{com} and tap strength, beginning with a uniform prior over (μ,σ), we used Bayes' rule to calculate the posterior probability over (μ,σ), which we marginalized to find the posterior over μ. We then calculated

$$p(\mu_{wk} > \mu_{str} \mid D_{wk}, D_{str}) = \int_{\mu_{str}} p(\mu_{str} \mid D_{str}) \left(\int_{\mu_{wk} > \mu_{str}} p(\mu_{wk} \mid D_{wk}) d\mu_{wk} \right) d\mu_{str} \quad (9)$$

Second, for each participant, we calculated the probability that τ in the weak-tap condition was greater than that in the strong-tap condition. For each participant, and separately for each tap strength condition, we discretized τ into bins of width 1.5 ms (bin midpoints: 1–151 ms) and calculated the posterior probability over each τ bin as the sum of posterior probabilities of all (σ_s, σ_v) for which σ_s/σ_v fell within the corresponding bin. We calculated shortest 95% credible intervals (95% CI) for each participant's τ in both the weak- and strong-tap conditions. Additionally, we calculated

$$p(\tau_{wk} > \tau_{str} \mid d_{wk}, d_{str}) = \sum_{\tau_{str}=1\mathrm{ms}}^{149.5\mathrm{ms}} p(\tau_{str} \mid d_{str}) \left(\sum_{\tau_{wk}=\tau_{str}+1.5\mathrm{ms}}^{151\mathrm{ms}} p(\tau_{wk} \mid d_{wk}) \right) \quad (10)$$

RESULTS

Weaker Taps Were Localized with Greater Uncertainty

We determined each participant's JND on length comparison blocks with t_{com} = 1,000 ms, separately for strong and weak taps. A paired *t*-test revealed that the JND was significantly larger in the weak tap condition (t_{19} = 3.207, P = 0.005). Expressed as a Weber fraction, the mean JND for the weak-tap condition was 90%, a value 1.7 times that for the strong-tap condition (54%) (Fig. 4*A*). Thus our manipulation of tap strength successfully elevated the participants' spatial uncertainty, as predicted from neural response considerations (Fig. 1*C*).

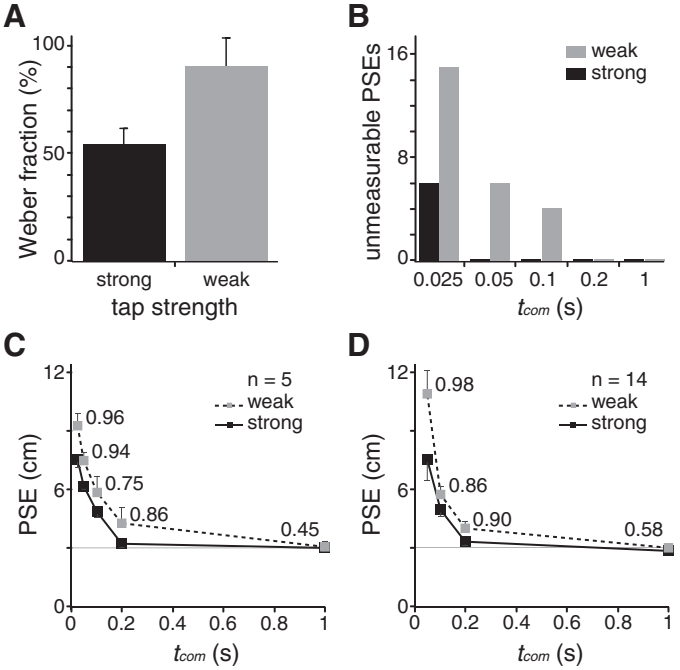

Fig. 4. Effects of tap strength. *A*: tap strength affects spatial uncertainty. Mean Weber fraction [just noticeable difference (JND) expressed as % increase from the reference] for discrimination between comparison and reference tap separations. Error bars show 1 SE. *B*: no. of participants with unmeasurable PSEs at each of the standard comparison times (t_{com} = 25, 50, 100, 200, and 1,000 ms) in strong-tap and weak-tap conditions. *C*: mean PSE at each t_{com} for strong- and weak-tap conditions. Only data from the 5 participants who had measurable PSEs at all comparison times are included in the average. The number above each weak-tap data point is the posterior probability that the PSE in the weak-tap condition was greater than that in the strong-tap condition. Error bars show +1 SE and −1 SE for weak and strong, respectively (when error bars are not visible, it is because they were smaller than the size of the data point square). Horizontal line: PSE = 3 cm (i.e., l_{ref}). *D*: as in *C* but showing data from the 14 participants who had measurable PSEs up to and including the 50 ms comparison time.

Weaker Taps Evoked More Pronounced Length Contraction

We next assessed participants' judgment of the distance between two spatially separated taps applied in rapid succession. In keeping with the predictions of the Bayesian model (Fig. 3*D*), participants consistently experienced *1*) a nonlinear growth in the degree of length contraction as comparison time was reduced and *2*) more pronounced length contraction when weak taps were used (Fig. 4, *B–D*).

Interestingly, length contraction was so pronounced in some cases that we could not move the comparison pair stimulators far enough apart to estimate a PSE (see MATERIALS AND METHODS), and this was particularly true in the weak-tap condition. In weak-tap experiments, 15 of 20 participants (75%) had unmeasurable PSEs at t_{com} = 25 ms, 6 (30%) had unmeasurable PSEs at t_{com} = 50 ms, and 4 (20%) had unmeasurable PSEs at t_{com} = 100 ms. The corresponding numbers in the strong-tap experiments were just 6, 0, and 0 participants, respectively (Fig. 4*B*).

Participants' measurable PSEs also revealed a stark difference between the strong- and weak-tap conditions. Among

participants who completed the full t_{com} range in both conditions ($n = 5$), the mean PSE at each $t_{com} < 1{,}000$ ms was consistently larger for the weak-tap condition than for the strong-tap condition (Fig. 4*C*). A 5 (t_{com}) × 2 (tap strength) repeated-measures ANOVA revealed significant main effects of t_{com} ($F_{4,16} = 48.737$, $P = 1 \times 10^{-8}$) and of tap strength ($F_{1,4} = 18.043$, $P = 0.013$) on PSE.

Similar results were found for the larger number of participants who had measurable PSEs in both conditions up to and including $t_{com} = 50$ ms ($n = 14$). Once again, the mean PSE at each $t_{com} < 1{,}000$ ms was consistently larger for the weak-tap condition than for the strong-tap condition (Fig. 4*D*). A 4 (t_{com}) × 2 (tap strength) repeated-measures ANOVA revealed significant main effects of t_{com} ($F_{1.2,15.8} = 35.996$, $P = 1 \times 10^{-5}$) and of tap strength ($F_{1,13} = 13.183$, $P = 0.003$) and a significant t_{com} × tap strength interaction ($F_{1.2,16.2} = 4.273$, $P = 0.048$), as predicted by the Bayesian model (Fig. 3*D*).

We next undertook a Bayesian analysis, separately at each t_{com}, to compare the posterior probability over the mean PSE in the weak-tap condition (μ_{wk}) to that in the strong-tap condition (μ_{str}). This analysis concluded confidently (probabilities ranging from 75% to 98%) that μ_{wk} exceeded μ_{str} at each t_{com} other than 1,000 ms (Fig. 4, *C* and *D*).

Human Performance Was Well Fit by the Bayesian Observer Model

As in the sample averages (Fig. 4), individual participants showed accelerating length contraction as t_{com} diminished, and they consistently tended to show more pronounced length contraction (larger PSE) at each t_{com} for the weak-tap condition than for the strong-tap condition (Fig. 5*A*). For each participant, separately for the weak and strong conditions, we found the model's best-fitting σ_s and σ_v values. The performance of the Bayesian observer matched that of the 20 humans with median r^2 values of 0.86 for both the strong-tap and weak-tap conditions (Fig. 5*B*).

The best-fit σ_s for weak stimuli was significantly greater than that for strong stimuli (paired *t*-test, $t_{19} = 4.094$, $P = 6 \times 10^{-4}$) (Fig. 6*A*). As expected for a measure of spatial uncertainty, the model-fit σ_s values correlated significantly with the JND values in both the weak-tap (Pearson's $r = 0.72$, $P = 0.0003$) and strong-tap (Pearson's $r = 0.50$, $P = 0.03$) conditions. A single participant had a strong-tap JND > 3 SD from the mean; the removal of that data point improved the correlation between the strong-tap JND and the model-fit σ_s values (Pearson's $r = 0.74$, $P = 0.0003$, $n = 19$).

As a further check that the model-fit σ_s values accurately reflected the participants' spatial uncertainty, we estimated each participant's σ_s exclusively from the data at $t_{com} = 1{,}000$ ms, using the model equations under the assumption that no length contraction occurs at 1,000 ms (i.e., setting $\tau/1{,}000$ ms, and equivalently τ/t_{com}, to 0 in *Eqs. 2*). Like the JND, these 1,000-ms σ_s estimates provided a measure of participants' spatial uncertainty in the absence of temporal manipulation. As expected, the 1,000-ms σ_s values did not differ significantly from the model-fit σ_s values (paired *t*-tests: weak tap, $t_{19} = 1.799$, $P = 0.09$; strong tap, $t_{19} = 1.335$, $P = 0.20$.).

In contrast to the model-fit σ_s values, there was no significant difference in model-fit σ_v values between the weak- and strong-tap conditions (paired *t*-test, $t_{19} = -0.359$, $P = 0.724$) (Fig. 6*B*). Consequently, the model-fit τ was significantly greater in the weak-tap condition than in the strong-tap condition (paired *t*-test, $t_{19} = 5.432$, $P = 3 \times 10^{-5}$) (Fig. 6*C*). The data permitted reasonably precise estimates of each participant's τ values. Among the 20 participants, the median span of the 95% CI for τ was 8 ms for the strong-tap condition and 19 ms for the weak-tap condition. Most importantly, the data supported the firm conclusion that the weak-tap τ was greater than the strong-tap τ in nearly all participants. The probability that the weak-tap τ was greater than the strong-tap τ exceeded 90% in 18 participants, 95% in 17 participants, and 99% in 16 participants.

Across the 20 participants, the mean σ_s for the weak-tap condition (2.11 cm) was 1.6 times that for the strong-tap condition (1.31 cm); similarly, the mean τ for the weak-tap condition (66 ms) was 1.7 times that for the strong-tap condition (39 ms). Thus

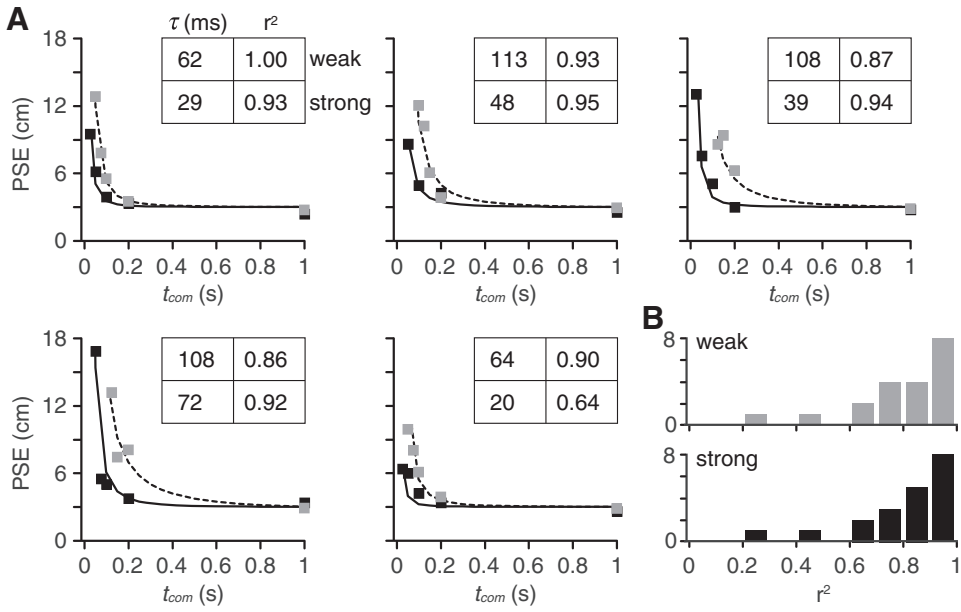

Fig. 5. Perceptual data and model fits. *A*: Bayesian observer fits to 5 individual participants. For each participant, PSE is plotted against t_{com}. Black squares, strong-tap condition; gray squares, weak-tap condition. Curves: PSEs of the Bayesian observer (solid: strong-tap condition; dashed: weak-tap condition). *Inset*: best-fit time constants (τ) and coefficients of variation between model fit and human data (r^2). *B*: histograms of r^2 values describing the Bayesian observer's fits to all 20 participants in the weak (*top*)- and strong (*bottom*)-tap conditions. Bins are 0.1 in width.

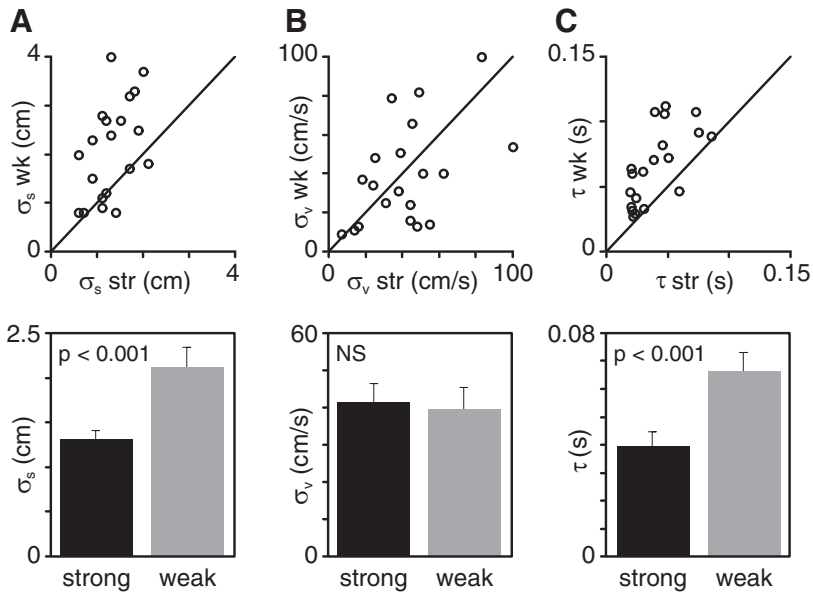

Fig. 6. Best-fit parameter values for the human participants. *Top*: Bayesian observer's parameter values that best fit each participant's data for strong (str) and weak (wk) tap conditions. *Bottom*: mean best-fit parameter values. Error bars: 1 SE. Paired *t*-test *P* values are shown; NS, not significant. *A*: σ_s. *B*: σ_v. *C*: τ.

perception became more susceptible to length contraction when weak taps were used.

DISCUSSION

Perception remarkably shrinks the distance between stimuli that occur in rapid succession. This phenomenon, dubbed perceptual length contraction (Goldreich 2007), has been most thoroughly studied in touch but occurs also in vision (Geldard 1976; Khuu et al. 2011; Lockhead et al. 1980) and audition (Bremer et al. 1977; Getzmann 2009; Shore et al. 1998). Tactile length contraction illusions have fascinated and puzzled researchers for more than 100 years (Asai and Kanayama 2012; Gelb 1914; Geldard and Sherrick 1972; Helson 1930; Kilgard and Merzenich 1995; Miyazaki et al. 2010; Trojan et al. 2014). We put forth a low-velocity-prior Bayesian observer model to explain length contraction, and we noted that our model made a novel prediction: that stimuli associated with greater spatial uncertainty would evoke more length contraction (Goldreich and Tong 2013). Here, in tactile psychophysical experiments with 20 participants, we confirmed that prediction.

Comparison to Previous Studies

We previously noted that length contraction is more pronounced on body sites that have poorer spatial acuity (Goldreich 2007). For instance, spatial acuity is known to worsen progressively from finger to forehead to forearm (Weinstein 1968). Our Bayesian model fit spatiotemporal perceptual data from these three sites (e.g., Cholewiak 1999; Marks et al. 1982) with progressively increasing τ values; this result led us to speculate that σ_v might be approximately constant across the body surface, such that τ grows in proportion to σ_s (Goldreich 2007). However, any conclusion based on cross-study comparisons is tentative because of differences in stimulus delivery, testing paradigms, and participants. In the present study, we directly confirmed the effect of σ_s on length contraction by manipulating stimulus strength in individual participants at a single body site. This is the first study to experimentally test our model.

Investigators can test Bayesian models by manipulating priors or likelihoods. An approach used to manipulate priors is to draw stimuli from a distribution that is novel to the participant. If participants' priors shift to conform to the new stimulus distribution, the Bayesian model predicts precisely how perception should change. While this approach has been successful in many instances (Adams et al. 2004; Knill 2007; Kording and Wolpert 2004; Vilares et al. 2012), it requires an adaptable prior. Series and Seitz (2013) categorized priors according to their malleability in the face of changing stimulus statistics: structural priors are perhaps learned over a lifetime of consistent experience and therefore difficult to change; contextual priors, in contrast, are readily adapted to new situations. We did not attempt here to manipulate the low-velocity prior, which we suspect may be resistant to change. Nevertheless, an interesting aspect of our model is that the low-velocity prior gives rise to a contextual prior over length; specifically, the time between taps provides a context that informs the prior over length, which widens in proportion to the product of t and σ_v (Fig. 2).

An approach used to manipulate likelihoods is to adjust stimulus clarity (signal-to-noise ratio). The Bayesian framework predicts that when stimuli are noisier (evoking broader likelihood functions), the percept will be more influenced by the prior. This prediction has been confirmed for several visual and auditory tasks (Fischer and Pena 2011; Girshick et al. 2011; Parise et al. 2014; Tassinari et al. 2006; Vilares et al. 2012; Weiss et al. 2002). Weiss et al. (2002) found that participants perceived low-contrast visual stimuli to move more slowly than high-contrast stimuli of equal velocity, consistent with the action of a low-velocity prior. Just as Weiss et al. (2002) varied visual stimulus contrast, here we varied tactile stimulus strength to evoke broader (weak taps) or sharper (strong taps) likelihood functions. We found that sequences of weak taps increased spatial uncertainty and resulted in more length contraction. This outcome is consistent with the perception of a Bayesian brain that operates with a low-velocity prior expectation.

An expected consequence of the low-velocity prior, as indicated by the perceptual length contraction formula (Fig. 2*B*), is that two brief simultaneously delivered stimuli ($t = 0$) will be perceived to occur at the same location ($l^* = 0$) midway between them. This phenomenon indeed occurs, as reported by Békésy (1957). Similarly, Wieland (1960) found that two brief, spatially separated stimuli to the forearm are perceived to occur at the same location when the time between them is made sufficiently short. Interestingly, and also consistent with our model (Goldreich 2007), when the distance separating stimuli was increased, shorter temporal intervals were required to produce the perception of spatial coincidence (Wieland 1960). These results may at first glance seem to conflict with the well-known ability of humans to distinguish the separation between two caliper points simultaneously applied to the skin, a test often used clinically, although criticized as an flawed measure of spatial acuity (Lundborg and Rosen 2004; Tong et al. 2013). Importantly, however, in such clinical tests the calipers are left resting on the skin for a prolonged period (on the order of 1 s). Our Bayesian model, in contrast, applies specifically to brief stimuli (e.g., Fig. 3*A*), which are consistent with the fleeting movement of a high-speed object.

Converging evidence from vision, audition, and touch suggests that the brain may generally apply a low-velocity prior to aid motion perception. Notably, in many experimental settings humans perceive noisier visual inputs to be slower moving (Jogan and Stocker 2015; Sotiropoulos et al. 2014; Weiss et al. 2002; Welchman et al. 2008), a phenomenon recently reported for auditory motion perception as well (Senna et al. 2015). Furthermore, the rabbit illusion occurs not only in touch but also in vision (Geldard 1976; Khuu et al. 2011; Lockhead et al. 1980) and audition (Bremer et al. 1977; Getzmann 2009; Shore et al. 1998), suggesting that a low-velocity prior may underlie the illusion in all three senses (Goldreich and Tong 2013); interestingly, the visual rabbit illusion is most pronounced in the periphery (Geldard 1976), where spatial acuity is poor, a feature easily understood in light of our model. Finally, tactile length contraction is evoked by smooth as well as punctate motion (Langford and Hall 1973; Seizova-Cajic and Taylor 2014; Whitsel et al. 1986); for instance, the fixed distance swept by a brush along the forearm is progressively underestimated as sweep velocity increases (Whitsel et al. 1986). These observations support the pervasive involvement of a low-velocity prior for motion perception; other expectations, such as a low-acceleration prior, may also come into play in certain contexts (Nguyen et al. 2016).

Future Directions

Here we assessed the perceived distance between taps but not the perceived positions of the individual taps in the stimulus sequence. Our model can predict the perceived positions of individual taps, and future experiments will test these predictions. Of particular interest will be experiments that test the perceptual effects of nonuniform spatial acuity. According to the model, when spatial acuity is uniform along the arm the perceived location of each tap will be symmetrically displaced toward the location of the other. In contrast, if spatial acuity is manipulated to be nonuniform, such that σ_s is less at one tap location than the other, the model predicts that length contraction will become asymmetric: the perceived trajectory's midpoint will shift toward the region of higher spatial acuity (see Fig. 8 and Eqs. 4 and 5 of Goldreich and Tong 2013).

Nonuniform spatial acuity could be achieved by using taps of different strength within a stimulus sequence, or perhaps by manipulating spatial attention. Interestingly, when participants direct attention preferentially to one location on the arm, spatial acuity reportedly increases there (i.e., σ_s decreases) (Moore et al. 1999; O'Boyle et al. 2001). Additionally, in the cutaneous rabbit paradigm, directed spatial attention has been shown to lessen the perceptual migration of the attended tap and to increase the perceptual migration of the unattended tap (Kilgard and Merzenich 1995). These results are in qualitative agreement with the predictions of our model. However, Kilgard and Merzenich (1995) did not measure the spatial acuity of their participants at the attended or unattended skin locations. Future length contraction studies could concomitantly measure σ_s at both locations in order to quantitatively test the model's predictions.

A direct manipulation of the tactile low-velocity prior has yet to be attempted. Future experiments could expose participants to frequent presentation of high-velocity stimulus trajectories, perhaps in conjunction with visual indicators of tap location, in an attempt to train expectation. Could such experiments increase σ_v or even shift the mode of the prior away from zero? In the former case, our model predicts that length contraction would weaken; in the latter case, the model predicts that slow movement would produce length expansion illusions. The low-velocity prior may prove to be resistant to short-term changes in stimulus statistics, if, as we suspect, it is built from a lifetime of accumulated experience. Nevertheless, the visual low-velocity prior has indeed been successfully manipulated in the laboratory (Sotiropoulos et al. 2011).

In the absence of information to the contrary, we have assumed for mathematical convenience that observers' low-velocity priors are Gaussian. Future experiments could attempt to extract the prior distributions (and likelihood functions) of individual participants, as accomplished in vision by Stocker and Simoncelli (2006). A necessary condition for the optimality of Bayesian inference is that the observer's prior match the environmental stimulus distribution (Girshick et al. 2011; Ma 2012). Some studies have measured natural visual and auditory scene statistics and found that humans perceive equivalently to a Bayesian observer that uses these distributions (Geisler and Perry 2009; Girshick et al. 2011; Parise et al. 2014). Analogous approaches in the tactile modality, although technically challenging, should be pursued.

Finally, experiments are needed to determine whether our model describes length contraction illusions in vision and audition equally well as it does in touch, and whether the model can be extended to explain temporal as well as spatial distortion illusions. We predict that visual and auditory experiments that are analogous to our tactile experiments will yield similar results, in which length contraction becomes more pronounced when punctate stimuli (light flashes or auditory beeps) are made more difficult to localize. Regarding temporal illusions, Goldreich (2007) showed that with the addition of a σ_t term to reflect temporal uncertainty, the Bayesian model can experience both length contraction and time dilation (the illusory expansion of the time between stimuli). Goldreich (2007) further showed, however, that on areas of the body with poor spatial acuity, such as the forearm, the model's length contrac-

tion was predominant and time dilation negligible, so that a Bayesian observer with temporal uncertainty perceived equivalently to one with veridical time perception; for that reason, here and in Goldreich and Tong (2013), we have conditioned on *t*. Future research will determine whether, as predicted by Goldreich (2007), time dilation illusions such as the kappa effect (Cohen et al. 1953; Suto 1952) are more pronounced on sensory regions that have finer spatial acuity (e.g., the fingertip and the fovea), where the balance of sensory uncertainty may shift from the spatial to the temporal domain.

Conclusions

The Bayesian framework formulates perception as a compromise between uncertain sensory data and expectation based in experience. A central prediction of this formulation is that when sensory data are less informative expectation will exert greater influence on the percept. Here we found that tactile perception conforms to this prediction. Specifically, stimulus sequences made from weaker taps elicited more perceptual length contraction, confirming our model's prediction that the low-velocity prior would exert greater influence under conditions of elevated spatial uncertainty. These findings support the view that the tactile percept is a probabilistic best guess resulting from a Bayesian inference process.

ACKNOWLEDGMENTS

We thank Maria Merlano for assistance with experiments and Keon Allen, Arnav Bharadwaj, Arindam Bhattacharjee, Tyler Czaniecki, Akash Deep, Luxi Li, Saba Saiel, Michael Wan, and Michael Wong for their comments on the manuscript.

Present address of J. Tong: Biological Psychology and Neuropsychology, Univ. of Hamburg.

Present address of V. Ngo: Dept. of Pathology and Laboratory Medicine, Western Univ.

GRANTS

This work was funded by a Discovery Grant to D. Goldreich from the Natural Sciences and Engineering Research Council of Canada (NSERC).

DISCLOSURES

No conflicts of interest, financial or otherwise, are declared by the author(s).

AUTHOR CONTRIBUTIONS

J.T., V.N., and D.G. conception and design of research; J.T. and V.N. performed experiments; J.T., V.N., and D.G. analyzed data; J.T., V.N., and D.G. interpreted results of experiments; J.T. and D.G. prepared figures; J.T. and D.G. drafted manuscript; J.T., V.N., and D.G. edited and revised manuscript; J.T., V.N., and D.G. approved final version of manuscript.

REFERENCES

Adams WJ, Graf EW, Ernst MO. Experience can change the "light-from-above" prior. *Nat Neurosci* 7: 1057–1058, 2004.

Asai T, Kanayama N. "Cutaneous rabbit" hops toward a light: unimodal and cross-modal causality on the skin. *Front Psychol* 3: 427, 2012.

Békésy G. Sensations on the skin similar to directional hearing, beats, and harmonics of the ear. *J Acoust Soc Am* 29: 489–501, 1957.

Blankenburg F, Ruff CC, Deichmann R, Rees G, Driver J. The cutaneous rabbit illusion affects human primary sensory cortex somatotopically. *PLoS Biol* 4: e69, 2006.

Bremer CD, Pittenger JB, Warren R, Jenkins JJ. An illusion of auditory saltation similar to the cutaneous "rabbit." *Am J Psychol* 90: 645–654, 1977.

Cholewiak RW. The perception of tactile distance: influences of body site, space, and time. *Perception* 28: 851–875, 1999.

Cholewiak RW, Collins AA. Vibrotactile localization on the arm: effects of place, space, and age. *Percept Psychophys* 65: 1058–1077, 2003.

Cody FW, Garside RA, Lloyd D, Poliakoff E. Tactile spatial acuity varies with site and axis in the human upper limb. *Neurosci Lett* 433: 103–108, 2008.

Cohen J, Hansel CE, Sylvester JD. A new phenomenon in time judgment. *Nature* 172: 901, 1953.

Fischer BJ, Pena JL. Owl's behavior and neural representation predicted by Bayesian inference. *Nat Neurosci* 14: 1061–1066, 2011.

Geisler WS, Kersten D. Illusions, perception and Bayes. *Nat Neurosci* 5: 508–510, 2002.

Geisler WS, Perry JS. Contour statistics in natural images: grouping across occlusions. *Vis Neurosci* 26: 109–121, 2009.

Gelb A. Versuche auf dem Gebiete der Zeit- und Raumanschauung. In: *Bericht über den VI. Kongress für experimentelle Psychologie in Göttingen April 1914*, edited by Schumann F. Leipzig, Germany: Barth, 1914, p. 36–42.

Geldard FA. The saltatory effect in vision. *Sens Processes* 1: 77–86, 1976.

Geldard FA. Saltation in somesthesis. *Psychol Bull* 92: 136–175, 1982.

Geldard FA, Sherrick CE. The cutaneous "rabbit": a perceptual illusion. *Science* 178: 178–179, 1972.

Getzmann S. Exploring auditory saltation using the "reduced-rabbit" paradigm. *J Exp Psychol* 35: 289–304, 2009.

Girshick AR, Landy MS, Simoncelli EP. Cardinal rules: visual orientation perception reflects knowledge of environmental statistics. *Nat Neurosci* 14: 926–932, 2011.

Goldreich D. A Bayesian perceptual model replicates the cutaneous rabbit and other tactile spatiotemporal illusions. *PLoS One* 2: e333, 2007.

Goldreich D, Tong J. Prediction, postdiction, and perceptual length contraction: a Bayesian low-speed prior captures the cutaneous rabbit and related illusions. *Front Psychol* 4: 221, 2013.

Helson H. The tau effect—an example of psychological relativity. *Science* 71: 536–537, 1930.

Jogan M, Stocker AA. Signal integration in human visual speed perception. *J Neurosci* 35: 9381–9390, 2015.

Khuu SK, Kidd JC, Badcock DR. The influence of spatial orientation on the perceived path of visual saltatory motion. *J Vis* 11: 5, 2011.

Kilgard MP, Merzenich MM. Anticipated stimuli across skin. *Nature* 373: 663, 1995.

Klein SA. Measuring, estimating, and understanding the psychometric function: a commentary. *Percept Psychophys* 63: 1421–1455, 2001.

Knill DC. Learning Bayesian priors for depth perception. *J Vis* 7: 13, 2007.

Knill DC, Pouget A. The Bayesian brain: the role of uncertainty in neural coding and computation. *Trends Neurosci* 27: 712–719, 2004.

Kontsevich LL, Tyler CW. Bayesian adaptive estimation of psychometric slope and threshold. *Vision Res* 39: 2729–2737, 1999.

Kording KP, Wolpert DM. Bayesian integration in sensorimotor learning. *Nature* 427: 244–247, 2004.

Langford N, Hall RJ. Cutaneous perception of a tract produced by a moving point across the skin. *J Exp Psychol* 97: 59–63, 1973.

Lechelt EC, Borchert R. The interdependence of time and space in somesthesis: the Tau effect reexamined. *Bull Psychon Soc* 10: 191–193, 1977.

Lockhead GR, Johnson RC, Gold FM. Saltation through the blind spot. *Percept Psychophys* 27: 545–549, 1980.

Lundborg G, Rosen B. The two-point discrimination test—time for a re-appraisal? *J Hand Surg Br* 29: 418–422, 2004.

Ma WJ. Organizing probabilistic models of perception. *Trends Cogn Sci* 16: 511–518, 2012.

Ma WJ, Beck JM, Latham PE, Pouget A. Bayesian inference with probabilistic population codes. *Nat Neurosci* 9: 1432–1438, 2006.

Marks LE, Girvin JP, Quest DO, Antunes JL, Ning P, O'Keefe MD, Dobelle WH. Electrocutaneous stimulation. II. The estimation of distance between two points. *Percept Psychophys* 32: 529–536, 1982.

Miyazaki M, Hirashima M, Nozaki D. The "cutaneous rabbit" hopping out of the body. *J Neurosci* 30: 1856–1860, 2010.

Moore CE, Partner A, Sedgwick EM. Cortical focusing is an alternative explanation for improved sensory acuity on an amputation stump. *Neurosci Lett* 270: 185–187, 1999.

Nguyen EH, Taylor JL, Brooks J, Seizova-Cajic T. Velocity of motion across the skin influences perception of tactile location. *J Neurophysiol* 115: 674–684, 2016.

O'Boyle DJ, Moore CE, Poliakoff E, Butterworth R, Sutton A, Cody FW. Human locognosic acuity on the arm varies with explicit and implicit manipulations of attention: implications for interpreting elevated tactile acuity on an amputation stump. *Neurosci Lett* 305: 37–40, 2001.

Parise CV, Knorre K, Ernst MO. Natural auditory scene statistics shapes human spatial hearing. *Proc Natl Acad Sci USA* 111: 6104–6108, 2014.
Penny W. Bayesian models of brain and behaviour. *ISRN Biomath* 2012: 1–19, 2012.
Peters RM, Staibano P, Goldreich D. Tactile orientation perception: an ideal observer analysis of human psychophysical performance in relation to macaque area 3b receptive fields. *J Neurophysiol* 114: 3076–3096, 2015.
Pizlo Z. Perception viewed as an inverse problem. *Vision Res* 41: 3145–3161, 2001.
Seizova-Cajic T, Taylor JL. Somatosensory space abridged: rapid change in tactile localization using a motion stimulus. *PLoS One* 9: e90892, 2014.
Senna I, Parise CV, Ernst MO. Hearing in slow-motion: humans underestimate the speed of moving sounds. *Sci Rep* 5: 14054, 2015.
Series P, Seitz AR. Learning what to expect (in visual perception). *Front Hum Neurosci* 7: 668, 2013.
Shadlen MN, Newsome WT. The variable discharge of cortical neurons: implications for connectivity, computation, and information coding. *J Neurosci* 18: 3870–3896, 1998.
Shore DI, Hall SE, Klein RM. Auditory saltation: a new measure for an old illusion. *J Acoust Soc Am* 103: 3730–3733, 1998.
Sotiropoulos G, Seitz AR, Series P. Changing expectations about speed alters perceived motion direction. *Curr Biol* 21: R883–R884, 2011.
Sotiropoulos G, Seitz AR, Series P. Contrast dependency and prior expectations in human speed perception. *Vision Res* 97: 16–23, 2014.
Sripati AP, Yoshioka T, Denchev P, Hsiao SS, Johnson KO. Spatiotemporal receptive fields of peripheral afferents and cortical area 3b and 1 neurons in the primate somatosensory system. *J Neurosci* 26: 2101–2114, 2006.
Stocker AA, Simoncelli EP. Noise characteristics and prior expectations in human visual speed perception. *Nat Neurosci* 9: 578–585, 2006.
Suto Y. The effect of space on time estimation (S-effect) in tactual space. *Shinrigaku Kenkyu* 22: 45–57, 1952.
Tassinari H, Hudson TE, Landy MS. Combining priors and noisy visual cues in a rapid pointing task. *J Neurosci* 26: 10154–10163, 2006.
Tong J, Mao O, Goldreich D. Two-point orientation discrimination versus the traditional two-point test for tactile spatial acuity assessment. *Front Hum Neurosci* 7: 579, 2013.
Trojan J, Heil M, Maihofner C, Holzl R, Kleinbohl D, Flor H, Benrath J. Spatiotemporal integration of tactile patterns along and across fingers. *Neuropsychologia* 53: 12–24, 2014.
Vilares I, Howard JD, Fernandes HL, Gottfried JA, Kording KP. Differential representations of prior and likelihood uncertainty in the human brain. *Curr Biol* 22: 1641–1648, 2012.
Vincent BT. A tutorial on Bayesian models of perception. *J Math Psychol* 66: 103–114, 2015.
Weinstein S. Intensive and extensive aspects of tactile sensitivity as a function of body part, sex, and laterality. In: *The Skin Senses: Proceedings*. Springfield, IL: Thomas, 1968, p. 195–222.
Weiss Y, Simoncelli EP, Adelson EH. Motion illusions as optimal percepts. *Nat Neurosci* 5: 598–604, 2002.
Welchman AE, Lam JM, Bulthoff HH. Bayesian motion estimation accounts for a surprising bias in 3D vision. *Proc Natl Acad Sci USA* 105: 12087–12092, 2008.
Whitsel BL, Franzen O, Dreyer DA, Hollins M, Young M, Essick GK, Wong C. Dependence of subjective traverse length on velocity of moving tactile stimuli. *Somatosens Res* 3: 185–196, 1986.
Wieland BA. The interaction of space and time in cutaneous perception. *Am J Psychol* 73: 248–255, 1960.
Yuille AL, Bülthoff HH. Bayesian decision theory and psychophysics. In: *Perception as Bayesian Inference*, edited by Knill DC, Richards W. Cambridge, UK: Cambridge Univ. Press, 1996.